

## Effect of Finite Radar Pulse Volume on Turbulence Measurements<sup>1</sup>

R. C. SRIVASTAVA AND D. ATLAS<sup>2</sup>

*Dept. of the Geophysical Sciences, The University of Chicago*

(Manuscript received 5 October 1973, in revised form 28 March 1974)

### ABSTRACT

Equations relating the mean of the Doppler spectrum and the distribution of point velocities, and their spectra are derived under the assumptions that: 1) the scatterers follow the air motion faithfully, 2) the reflectivity is constant, and 3) the beam illumination function is separable. It is found that the three-dimensional spectral density function is strongly attenuated at scales small compared to the beam dimensions, and essentially unaffected at scales large compared to the beam dimensions. Relationships between the one-dimensional longitudinal and transverse spectra of the mean velocity and the three-dimensional spectrum of the point velocities are derived. Numerical computations with a model Kolmogorov-Obukhov turbulence spectrum are performed to illustrate the effects of filtering. Energy at scales small compared to the beam dimensions is attenuated. Energy at scales large compared to the beam dimensions is also reduced, in the case of the one-dimensional spectrum, because small scales in the orthogonal directions contributing to the energy are attenuated by the filtering. The energy depleted from the spectrum of the mean velocity appears as an increased variance of the Doppler spectrum. The ratio of the total energy under the measured spectrum to that under the spectrum of the point velocities is computed as a function of beam dimensions. An equivalent rectangular filter approximation is proposed for computing the one-dimensional spectra. Analytical results are obtained for the longitudinal spectrum and are shown to be in excellent agreement with the numerical results for the actual filter. The use of a spherical volume equal to that of the actual radar pulse volume is shown to be invalid.

### 1. Introduction

A pulsed Doppler radar effectively measures the distribution of radial velocities of the scattering particles present in the radar pulse volume; this information is contained in the Doppler power spectrum. The mean of the Doppler power spectrum, called the mean Doppler velocity, is a weighted average of the radial velocities of the scatterers in the radar beam. It would seem, therefore, that some properties of the field of air motion and, in particular, that of the field of turbulence may be deduced from measurements of the mean Doppler velocity. Indeed, it has been demonstrated by a number of workers that the intensity and spectrum of turbulence and its associated structure function can be measured not only by Doppler radar (Mel'nichuk, 1966; Gorelik *et al.*, 1958, 1963; Lhermitte, 1968; Chernikov *et al.*, 1969) but also by incoherent radar

(Gorelik *et al.*, 1963; Mel'nichuk *et al.*, 1968; Atlas and Srivastava, 1971).

Ideally, in measuring the field of air motion, or turbulence, one would like to measure the point air velocities. Doppler radar measurements differ from this ideal, in two respects: 1) the radial velocity of the tracers may differ from that of the air because of the intrinsic motions of the scatterers, and 2) the measured mean Doppler velocity is an average over the pulse volume rather than a point value. This paper is concerned with the effects of the pulse-volume averaging and the consequent differences between the measured spectrum, and other properties of the turbulent velocity field, and the corresponding quantities for the point (unaveraged) velocity field. In order to clearly bring out the effects of pulse-volume averaging (also referred to as pulse-volume filtering), ideal tracers which follow the air motion perfectly will be assumed.

It is intuitively clear that one effect of pulse-volume averaging on the mean Doppler velocity is to smooth fluctuations on scales smaller than the pulse volume. Rogers and Tripp (1964) showed that the time variations of the mean Doppler velocity (in the case of a fixed beam) were related to the turbulent kinetic energy in eddies of scales larger than the pulse volume, and that the energy in scales smaller than the pulse volume appeared in the variance of the Doppler spectrum.

<sup>1</sup> Research supported by the Office of Naval Research under Contract N00014-67A-0285-0014 and the National Science Foundation under Grant NSF-GA-27680X. A shorter version of this paper appears in the Preprints of the 15th Radar Meteorology Conference, Champaign-Urbana, Ill., 10-12 October 1972; this paper has also been published as Tech. Rept. No. 27 of the Laboratory for Atmospheric Probing, The University of Chicago and Illinois Institute of Technology.

<sup>2</sup> Present affiliation: National Center for Atmospheric Research, Boulder, Colo. 80302.

They thus recognized the averaging effects of the pulse volume. Rogers and Tripp gave equations for the relationship between the spectra of the averaged and point velocities. However, they approximated the actual pulse volume by an idealized volume of simpler geometry. Gorelik *et al.* (1963) made a similar assumption.

In this paper, we consider the effects of averaging by the actual pulse volume. It will be shown that the substitution of the actual pulse volume by one of simpler geometry is not generally permissible. We shall also show, contrary to the conclusions of Rogers and Tripp, that pulse-volume filtering may also significantly reduce the turbulent spectral density at scales much larger than the pulse volume.

The considerations presented in this paper are generally relevant to the interpretation of observations where a finite sampling volume is used for the measurement of velocity (or some other property), as for example in the observations of Lhermitte (1968), Wilson (1970) and others. Radar observations of turbulence spectra are in progress at the Laboratory for Atmospheric Probing and one of the objectives of this study is to assess the effects of the pulse-volume filtering on the measured spectra. The inverse problem of recovering the unfiltered spectrum from that measured has been treated by Sychra (1972).

## 2. Description of turbulence

We begin with a brief review of some basic definitions and results relating to the description of turbulence. For detailed discussion and proofs of statements made in this section reference may be made to Batchelor (1953) or Tatarski (1961).

The turbulent air velocity  $\mathbf{v}(\mathbf{r})$  is a random function of position  $\mathbf{r}$  in space. We assume that the velocity field has zero mean and is statistically homogeneous. The spectral power density tensor function  $\phi_{ij}(\mathbf{k})$  [where  $\mathbf{k}$  is the vector wavenumber] is the Fourier transform of the correlation tensor function  $B_{ij}(\mathbf{r})$  of the velocity field. The Fourier transform of  $\mathbf{v}$  itself does not exist, but formally it may be written as a stochastic Fourier-Stieltjes integral

$$v_i(\mathbf{r}) = \int e^{j\mathbf{k} \cdot \mathbf{r}} dZ_i(\mathbf{k}), \tag{2.1}$$

with

$$\phi_{ij}(\mathbf{k}) = \lim_{d\mathbf{k} \rightarrow 0} \frac{\langle dZ_i^*(\mathbf{k}) dZ_j(\mathbf{k}) \rangle}{d\mathbf{k}}, \tag{2.2}$$

where the asterisk denotes the complex conjugate.

The longitudinal velocity correlation function  $B_L$  is obtained if both velocity components are along the direction of  $\mathbf{r}$ , and the transverse correlation function  $B_T$  is obtained if both velocity components are along a direction perpendicular to  $\mathbf{r}$ . The corresponding

longitudinal and transverse spectral density functions,  $\phi_L$  and  $\phi_T$  respectively, are obtained by integrating the three-dimensional spectrum function:

$$\phi_L(k_1) = \int \phi_{11}(\mathbf{k}) dk_2 dk_3, \tag{2.3}$$

$$\phi_T(k_2) = \int \phi_{11}(\mathbf{k}) dk_1 dk_3. \tag{2.4}$$

The form of the three-dimensional spectral function is particularly simple if the velocity field is statistically homogeneous and isotropic and the flow is incompressible. In this case

$$\phi_{ij}(\mathbf{k}) = \left( \delta_{ij} - \frac{k_i k_j}{k^2} \right) \frac{E(k)}{4\pi k^2}, \tag{2.5}$$

where  $E(k)$ , the energy spectrum function is such that  $E(k)dk$  is the contribution to the kinetic energy from wavenumbers of magnitude  $k$  to  $k+dk$ .

## 3. Pulse-volume filtering

In this section we discuss the relationship between the pulse-volume averaged velocity and the point velocity. Since the pulse-volume averaged velocity is in practice the mean of the Doppler spectrum, we shall first derive the relationship between the mean of the Doppler spectrum and the point velocity. Using this equation, we shall derive the desired relation between the spectra of the pulse-volume averaged and the point velocities.

### a. Doppler spectrum

The Doppler power spectrum  $S(v, \mathbf{r})$  is such that  $S(v, \mathbf{r})dv$  is equal to the average power returned by scatterers in the pulse volume, centered at  $\mathbf{r}$ , having radial velocities in the range  $v$  to  $v+dv$ . Let  $g(v, \mathbf{r})$  be the radar reflectivity density such that  $g(v, \mathbf{r})dv d\mathbf{r}$  is the radar cross section of the scatterers in the volume  $d\mathbf{r}$  in the velocity range  $v$  to  $v+dv$ . Since the velocity is a single-valued function of position, it is clear that  $g(v, \mathbf{r})=0$  unless  $v=v(\mathbf{r})$ , the velocity at the point  $\mathbf{r}$ . This may be expressed by writing  $g$  in terms of the Dirac delta function; i.e.,

$$g(v, \mathbf{r}) = \eta(\mathbf{r})\delta[v - v(\mathbf{r})], \tag{3.1}$$

where  $\eta(\mathbf{r})$  is the radar reflectivity. Let  $I(\mathbf{r}, \mathbf{R})$  be the two-way radar beam illumination function at the point  $\mathbf{R}$ . The illumination function is considered normalized, which is to say that

$$\int I(\mathbf{r}, \mathbf{R}) d\mathbf{R} = 1. \tag{3.2}$$

The Doppler power spectrum,  $S(v, \mathbf{r})$ , is now by definition

$$S(v, \mathbf{r}) = c_1 \int g(v, \mathbf{R}) I(\mathbf{r}, \mathbf{R}) d\mathbf{R}, \quad (3.3)$$

where  $c_1$  is a constant of proportionality depending upon the radar equipment. The mean of the Doppler spectrum,  $\bar{v}(\mathbf{r})$ , is given by

$$\bar{v}(\mathbf{r}) = \int v S(v, \mathbf{r}) dv / \int S(v, \mathbf{r}) dv, \quad (3.4)$$

$$= \int v g(v, \mathbf{R}) I(\mathbf{r}, \mathbf{R}) d\mathbf{R} dv / \int g(v, \mathbf{R}) I(\mathbf{r}, \mathbf{R}) d\mathbf{R} dv, \quad (3.5)$$

where we have substituted from (3.3) in (3.5). Carrying out the integrations in (3.5) with respect to  $v$  and making use of (3.1), we have

$$\bar{v}(\mathbf{r}) = \int \eta(\mathbf{R}) v(\mathbf{R}) I(\mathbf{r}, \mathbf{R}) d\mathbf{R} / \int \eta(\mathbf{R}) I(\mathbf{r}, \mathbf{R}) d\mathbf{R}. \quad (3.6)$$

In addition to the mean Doppler velocity, the area under the spectrum, which is equal to the average power received, may be measured. Through the constant of proportionality  $c_1$ , the power may be expressed as an average reflectivity  $\bar{\eta}(\mathbf{r})$  at the center  $\mathbf{r}$  of the pulse volume:

$$c_1 \cdot \bar{\eta}(\mathbf{r}) = \int S(v, \mathbf{r}) dv. \quad (3.7)$$

Again, substituting from (3.3) and integrating with respect to  $v$  with the help of (3.1), we get

$$\bar{\eta}(\mathbf{r}) = \int \eta(\mathbf{R}) I(\mathbf{r}, \mathbf{R}) d\mathbf{R}. \quad (3.8)$$

Thus, the measured reflectivity  $\bar{\eta}(\mathbf{r})$  is an average of the point reflectivity weighted by the beam illumination function. Combining (3.6) and (3.8) we have

$$\bar{\eta}(\mathbf{r}) \cdot \bar{v}(\mathbf{r}) = \int \eta(\mathbf{R}) v(\mathbf{R}) I(\mathbf{r}, \mathbf{R}) d\mathbf{R}. \quad (3.9)$$

For the sake of simplicity, we shall assume that  $\eta(\mathbf{R})$  is constant. Eq. (3.9) then simplifies to

$$\bar{v}(\mathbf{r}) = \int v(\mathbf{R}) I(\mathbf{r}, \mathbf{R}) d\mathbf{R}, \quad (3.10)$$

which says that, as in the case of the reflectivity, the mean of the Doppler spectrum is an average of the point radial velocities weighted by the beam illumination function.

It is clear from (3.10) that, at least in principle,  $v(\mathbf{R})$  can be deduced from measured  $\bar{v}(\mathbf{R})$  provided

the beam illumination function is known. However, our concern here is to deduce the spectral density function of  $v(\mathbf{r})$  from that of  $\bar{v}(\mathbf{r})$ .

#### b. Spectra of point and average velocities

It will now be assumed that the beam illumination function  $I(\mathbf{r}, \mathbf{R})$  depends only on  $\mathbf{r} - \mathbf{R}$ . This involves a certain approximation which is discussed below. With this assumption (3.10) may be rewritten as

$$\bar{v}(\mathbf{r}) = \int v(\mathbf{R}) I(\mathbf{r} - \mathbf{R}) d\mathbf{R}, \quad (3.11)$$

Thus, the pulse-volume averaged velocity is a convolution of the point velocity and the beam illumination function. Taking the Fourier transform of each side of (3.11), we have

$$dZ_{\bar{v}}(\mathbf{r}) = (2\pi)^3 dZ_v(\mathbf{k}) F_I(\mathbf{k}), \quad (3.12)$$

where  $F_I$  is the Fourier transform of the beam illumination function. Multiplying (3.12) by its complex conjugate, dividing by  $d\mathbf{k}$ , and taking limits, we have

$$\phi_{\bar{v}}(\mathbf{k}) = \phi_v(\mathbf{k}) \cdot \phi_I(\mathbf{k}), \quad (3.13)$$

where

$$\phi_I(\mathbf{k}) = (2\pi)^6 |F_I(\mathbf{k})|^2, \quad (3.14)$$

and  $\phi_{\bar{v}}$  and  $\phi_v$  are the power spectral densities of  $\bar{v}$  and  $v$ , respectively;  $\phi_I$  will be called the beam filter function. Eq. (3.13) gives the desired relation between the three-dimensional spectra of  $\bar{v}$  and  $v$ .

The spectrum  $\phi_v$  of the point radial velocity may be related to the spectral density tensor  $\phi_{ij}$  introduced in Section 2. Let the beam direction be  $x_1$  and suppose that the beam width of the radar is small, then the divergence of radial velocities may be ignored, and we have

$$\phi_v(\mathbf{k}) = \phi_{11}(\mathbf{k}). \quad (3.15)$$

According to Eqs. (3.13) and (3.15) then,  $\phi_{11}$  may be deduced if  $\phi_{\bar{v}}(\mathbf{k})$  is measured and  $\phi_I$  is known. To compute  $\phi_{\bar{v}}(\mathbf{k})$ ,  $\bar{v}$  itself must be measured as a function of  $\mathbf{r}$ . In practice, however,  $\bar{v}$  is measured as a function of  $x_1$  (beam direction), or as a function of  $x_2$ , a direction perpendicular to  $x_1$  and directed along the mean wind. The former measurement can be made simply by finding the mean Doppler velocities as a function of range while holding the antenna fixed. The latter measurement can be made by keeping the radar sampling volume fixed and measuring the mean radial velocity as a function of time as different parcels of air are swept through the beam. The time variation may then be converted to space ( $x_2$ ) variation knowing the wind speed and assuming Taylor's hypothesis.

From the first mode of measurement, we get the longitudinal one-dimensional spectrum of the mean

velocity,  $S_L(k_1)$ . By analogy to (2.3), we have

$$\begin{aligned}
 S_L(k_1) &= \int \phi_{\bar{v}}(\mathbf{k}) dk_2 dk_3, \\
 &= \int \phi_{11}(\mathbf{k}) \cdot \phi_I(\mathbf{k}) dk_2 dk_3, \tag{3.16}
 \end{aligned}$$

using (3.13) and (3.15). Similarly, in the second mode of operation, we obtain the transverse one-dimensional spectrum,  $S_T(k_2)$ , of  $\bar{v}$ . By analogy with (2.4) we have

$$\begin{aligned}
 S_T(k_2) &= \int \phi_{\bar{v}}(\mathbf{k}) dk_1 dk_3, \\
 &= \int \phi_{11}(\mathbf{k}) \phi_I(\mathbf{k}) dk_1 dk_3. \tag{3.17}
 \end{aligned}$$

It may be seen from (3.16) and (3.17) that  $\phi_{11}(\mathbf{k})$  cannot be uniquely determined from a measurement of  $S_L(k_1)$  or  $S_T(k_2)$  given the beam filter function  $\phi_I(\mathbf{k})$  unless some restrictions are placed on the form of  $\phi_{11}$ . One such set of restrictions are the assumptions of isotropy and incompressibility which relate  $\phi_{11}(\mathbf{k})$  to one function  $E(k)$  through (2.5). The inverse problem of determining  $E(k)$  from  $S_L$  or  $S_T$  under these restrictions is discussed by Sychra (1972). Here we shall confine ourselves to the direct problem of determining the effects of filtering by integration of (3.16) and (3.17). For this purpose, we first need to determine the beam filter function  $\phi_I(\mathbf{k})$ .

**4. Beam filter function**

The normalized two-way beam illumination function may be written as the product of a function of the coordinate along the beam direction,  $x_1$ , and another function of the coordinates  $(x_2, x_3)$  perpendicular to the beam direction, i.e.,

$$I(\mathbf{x}, \mathbf{X}) = I_2(x_2, x_3, X_2, X_3) I_1(x_1, X_1). \tag{4.1}$$

For a pulsed radar, the illumination function along the beam direction may be taken as rectangular, that is,

$$I_1(x_1, X_1) = \begin{cases} \frac{1}{c}, & |x_1 - X_1| < \frac{c}{2} \\ 0, & |x_1 - X_1| \geq \frac{c}{2} \end{cases} \tag{4.2}$$

where  $c = h/2$ ,  $h$  being the pulse length in space. The illumination function perpendicular to the beam direction may generally be well approximated by a Gaussian function

$$\begin{aligned}
 &I_2(x_2, x_3, X_2, X_3) \\
 &= \frac{1}{2\pi\sigma_2\sigma_3} \exp\left[-\frac{(x_2 - X_2)^2}{2\sigma_2^2} - \frac{(x_3 - X_3)^2}{2\sigma_3^2}\right], \tag{4.3}
 \end{aligned}$$

where

$$\sigma_i = \frac{X_1 \theta_i}{(8 \ln 4)^{\frac{1}{2}}} = \frac{B_i}{(8 \ln 4)^{\frac{1}{2}}} = 0.3003 B_i, \quad i = 2, 3, \tag{4.4}$$

and  $\theta_2$  and  $\theta_3$  are the half-power full beam widths in the  $x_2, x_3$  directions and  $B_2, B_3$  are the corresponding linear dimensions of the beam.

From the above equations, it is clear that the assumption made in Section 3.2 that  $I(\mathbf{r}, \mathbf{R})$  depends only on  $\mathbf{r} - \mathbf{R}$  is not rigorously satisfied because  $\sigma_2$  and  $\sigma_3$  depend on  $X_1$ . Of the two modes of operation mentioned in the previous section, it is not difficult to see that this dependence does not give rise to any errors in the mode involving the measurement of the transverse spectrum since  $X_1$  is kept fixed in this case. However, the assumption gives rise to errors in the mode involving the measurement of the longitudinal spectrum since  $X_1$  is varied in this case. But the error will be small if the total variation of  $X_1$  is small compared to its mean value. Henceforth we shall assume that  $\sigma_i$  and  $B_i$  are constants.

Carrying out the necessary Fourier transforms, it is found that

$$\begin{aligned}
 \phi_I(\mathbf{k}) &= \left[ \frac{\sin(k_1 c/2)}{(k_1 c/2)} \right]^2 \cdot \exp[-\sigma_2^2 k_2^2] \\
 &\quad \cdot \exp[-\sigma_3^2 k_3^2], \\
 &= \phi_1 \cdot \phi_2 \cdot \phi_3. \tag{4.5}
 \end{aligned}$$

We see that the three-dimensional filter function corresponding to the pulse volume is comprised of the product of three one-dimensional functions:  $\phi_1$  corresponding to the averaging of the velocity fluctuations along the  $x_1$  direction by the rectangular pulse has the form of a  $[(\sin u)/u]^2$  filter in the  $k_1$  direction, where  $u = k_1 c/2$ ;  $\phi_2$  and  $\phi_3$  associated with the averaging of velocity fluctuations in the  $x_2$  and  $x_3$  directions respectively have the form of Gaussian filters  $\exp(-\sigma_i^2 k_i^2)$  in the  $k_2$  and  $k_3$  directions because the beam illumination functions are Gaussian in the  $x_2$  and  $x_3$  directions. Clearly, the narrower the beamwidths, the smaller are  $\sigma_2$  and  $\sigma_3$  [Eq. (4.4)] and the wider are the associated filters in  $k_2$  and  $k_3$  directions, and so the greater will be the energy passed in the large wavenumbers or small scales. Similarly, as the pulse width is reduced, averaging in the  $x_1$  direction is limited to smaller and smaller scales, and so more small-scale or large  $k_1$  wavenumber energy is passed without loss.

A plot of  $\phi_1$  and  $\phi_2$  is shown in Fig. 1. It is seen that scales large compared to the pulse dimensions, that is, scales satisfying  $(L_2, L_3) \gg (B_2, B_3)$  and  $L_1 \gg c$  are essentially unaffected by the filtering. Scales small compared to the beam dimensions are severely attenuated. In order that  $\phi_1, \phi_2$  and  $\phi_3$  are each greater than 0.8, so that their product is greater than 0.5, we must have  $L_1 > 4c$  and  $(L_2, L_3) > 4(B_2, B_3)$ .

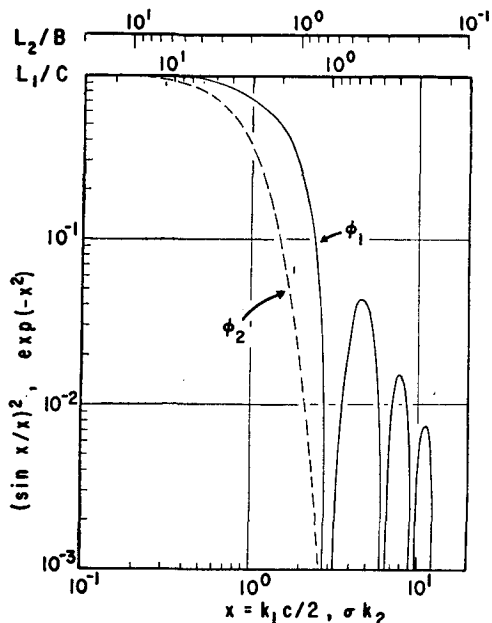


FIG. 1. Beam filter function.

Substituting (4.5) into (3.14), we have

$$\phi_{\bar{s}}(\mathbf{k}) = \phi_s(\mathbf{k}) \left[ \frac{\sin(k_1 c/2)}{(k_1 c/2)} \right]^2 \exp[-\sigma_2^2 k_2^2 - \sigma_3^2 k_3^2]. \quad (4.6)$$

Substituting into (3.17) and (3.18), we have

$$S_L(k_1) = \left[ \frac{\sin(k_1 c/2)}{(k_1 c/2)} \right]^2 \int \phi_{11}(\mathbf{k}) \times \exp(-\sigma_2^2 k_2^2 - \sigma_3^2 k_3^2) dk_2 dk_3, \quad (4.7)$$

$$S_T(k_2) = \exp(-\sigma_2^2 k_2^2) \int \phi_{11}(\mathbf{k}) \left[ \frac{\sin(k_1 c/2)}{(k_1 c/2)} \right]^2 \exp(-\sigma_3^2 k_3^2) dk_1 dk_3. \quad (4.8)$$

These equations explicitly show the dependence of  $S_L$  and  $S_T$  on the pulse volume dimensions and the spectrum  $\phi_{11}$  of the point velocities.

It is to be noted that the one-dimensional spectral density in a particular direction is degraded even though there may not be any filtering in that direction. Thus, referring to (4.7), we see that even with  $c=0$  (no filtering in  $k_1$  direction),  $S_L(k_1)$  is degraded due to filtering in the orthogonal  $(k_2, k_3)$  directions. This is because the one-dimensional spectral density at any wavenumber  $k_1$  is obtained by integration over all  $(k_2, k_3)$  after attenuating the three-dimensional spectral density by the beam filter functions in the  $(k_2, k_3)$  directions.

5. Results of numerical calculations

In order to quantitatively illustrate the effects of beam filtering on measured one-dimensional spectra,

we need to assume a model for  $\phi_{11}$ . We assume that the turbulence is isotropic and incompressible. In this case, we have from (2.5)

$$\phi_{11}(\mathbf{k}) = \left( 1 - \frac{k_1^2}{k^2} \right) \frac{E(k)}{4\pi k^2}. \quad (5.1)$$

For  $E(k)$ , we assume the Kolmogorov-Obukhov spectrum, with cutoff at a certain wavenumber  $k_0$ :

$$E(k) = \begin{cases} A \frac{\pi}{k^n}, & n = 5/3, \quad k > k_0 \\ 0, & k < k_0 \end{cases} \quad (5.2)$$

where  $A$  is a constant taken as 1 in the numerical calculations. The factor  $\pi$  is inserted for convenience in analytical manipulations. The cutoff is assumed so that the total energy under the spectrum is finite. In all the numerical calculations, a circular beam is assumed so that  $\sigma = \sigma_2 = \sigma_3$  and  $B = B_2 = B_3$ .

It may be shown that with (5.2) the longitudinal and transverse one-dimensional spectra of the point velocities are given by

$$\phi_L(k_1) = \begin{cases} A \frac{9\pi}{55} \frac{1}{k_1^{5/3}}, & k_1 > k_0 \\ A \frac{3\pi}{10} \frac{1}{k_0^{5/3}} \left[ 1 - \frac{5}{11} \left( \frac{k_1}{k_0} \right)^2 \right], & k_1 < k_0 \end{cases} \quad (5.3)$$

$$\phi_T(k_2) = \begin{cases} A \frac{12\pi}{55} \frac{1}{k_2^{5/3}}, & k_2 > k_0 \\ A \frac{3\pi}{20} \frac{1}{k_0^{5/3}} \left[ 1 + \frac{5}{11} \left( \frac{k_2}{k_0} \right)^2 \right], & k_2 < k_0. \end{cases} \quad (5.4)$$

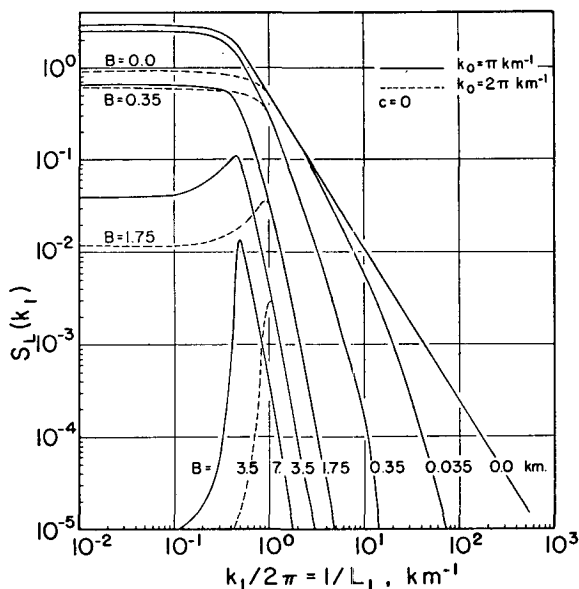


FIG. 2. Filtered longitudinal one-dimensional spectrum function.

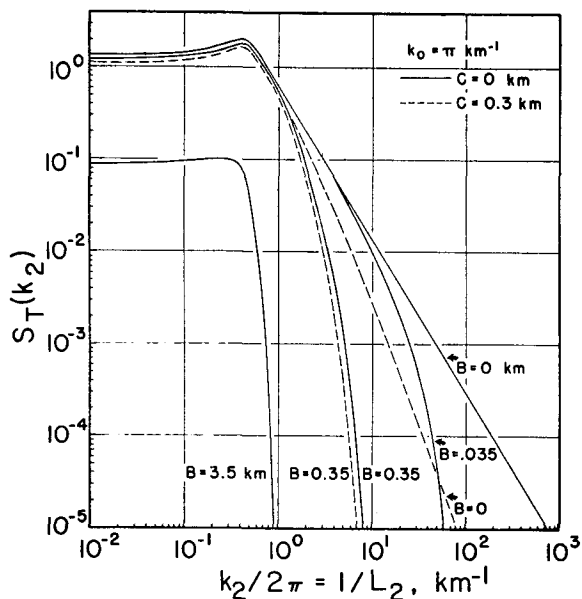


FIG. 3. Filtered transverse one-dimensional spectrum function.

The longitudinal one-dimensional spectrum computed from (4.7) and (5.1) is shown in Fig. 2, for two values of  $k_0$ , namely,  $\pi$  (full lines) and  $2\pi$  (dashed lines) corresponding to cutoff length scales of 2 and 1 km respectively,  $c=0$ , and various values of  $B$ . Results for other values of  $c$  may be obtained simply by multiplying the curves by  $\phi_1 = [\sin(k_1 c/2)/(k_1 c/2)]^2$ . For  $B=0, c=0$ , we have the unfiltered spectrum (5.3) obeying the  $\frac{5}{3}$ rd power law for  $k_1 > k_0$ . It is seen that the one-dimensional spectrum contains energy at wavenumbers smaller than, or scales larger than, the cutoff wavenumber. This is because at  $k_1 < k_0$  energy is contributed by scales  $(k_1, k_2, k_3)$  such that  $k_1^2 + k_2^2 + k_3^2 > k_0^2$ ; that is, by wavenumbers larger than  $k_0$  whose projection along the  $k_1$  axis is smaller than  $k_0$ . Keeping this interpretation in mind, it may be seen why the full and dashed curves differ only at the smaller wavenumbers with the dashed curves having the smaller energy.

Fig. 3 shows the transverse one-dimensional spectra for  $k_0 = \pi$  [ $\text{km}^{-1}$ ]. The curve for  $c=0, B=0$  follows the  $\frac{5}{3}$ rd law above  $k_2 > k_0$ . Note the considerable difference between the curves for  $B=0, c=0$  and  $B=0, c=0.3$  km. The difference between  $c=0$  and  $c=0.3$  km at  $B=0.35$  km is small and at  $B=3.5$  km it cannot be shown on the scale of the graph. This is because when the horizontal beam dimension becomes large compared to its vertical dimension, the filtering due to the latter may be ignored.

One quantity of interest is the total turbulent energy or the area under the spectral curve. Some investigators have used the turbulent energy for deducing the eddy dissipation rate, assuming an inertial subrange. The areas under the spectra have been numerically computed and are presented in Fig. 4 as contours of the

ratio of the filtered to the unfiltered energy. It is seen that with  $k_0 = 2\pi$  [ $\text{km}^{-1}$ ], both  $c$  and  $B$  should be less than about 80 m in order that 90% of the turbulent energy may be measured. Under the same conditions a smaller percentage of the energy is measured when  $k_0 = 2\pi$  [ $\text{km}^{-1}$ ]. This is because the smaller wavenumbers are essentially unattenuated, and there is more energy at the smaller wavenumbers with  $k_0 = \pi$  [ $\text{km}^{-1}$ ] than with  $k_0 = 2\pi$  [ $\text{km}^{-1}$ ]. It is seen that the contours become almost vertical as  $B$  increases; again, this is because with  $B$  large compared to  $c$ , the filtering action of the  $c$ -direction may be ignored.

Some authors (for example, Gorelik *et al.*, 1963) have suggested using an equivalent spherical volume of radius  $R$  given by

$$\frac{4\pi}{3} R^3 = \frac{\pi B^2}{4} c,$$

or

$$R = (3B^2 c / 16)^{1/3},$$

to estimate the effects of filtering. According to this approximation, the effects of filtering should be the same along lines of constant  $B^2 c$ . It is clear from Fig. 4 that such a simple rule is not valid.

### 6. Equivalent rectangular filter approximation

In the previous section, we have shown the effects of filtering by performing numerical integrations. In general, it is difficult to see the effects of filtering without numerical calculations. However, approximation of the actual beam filters by equivalent rectangular filters enables analytical results to be obtained in the case of the longitudinal spectrum. Moreover, in many

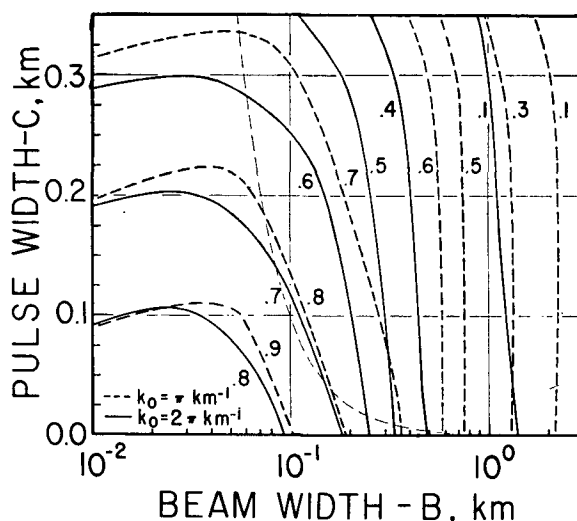


FIG. 4. Contours of the ratio of filtered to unfiltered turbulent kinetic energy as a function of pulse and beamwidth. The dash-dot line is a line of constant  $B^2 c$ , i.e., a line of constant pulse volume.

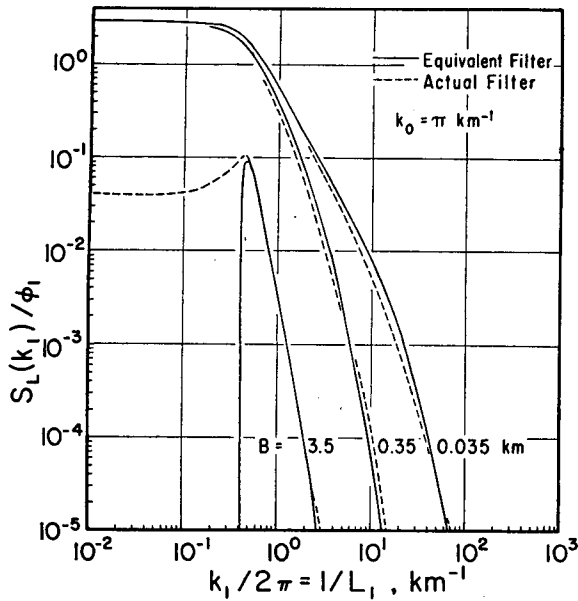


FIG. 5. Spectra with actual and equivalent filters.

cases the equivalent filters give spectra which are very similar to those computed from the actual filters. The equivalent rectangular filter approximation is therefore of great practical value.

The equivalent filters are defined as follows:

$$\phi_1'(k_1) = \begin{cases} 1, & |k_1| < k_{1e} \\ 0, & |k_1| \geq k_{1e} \end{cases} \quad (6.1)$$

$$\phi_2' \cdot \phi_3' = \begin{cases} 1, & |\rho| < \rho_e \\ 0, & |\rho| \geq \rho_e \end{cases} \quad (6.2)$$

where  $\rho^2 = k_2^2 + k_3^2$ , and a circular beam is assumed, i.e.,  $\sigma = \sigma_2 = \sigma_3$ . These filters are low-pass filters, their widths  $k_{1e}$  and  $\rho_e$  being determined so that the areas under the actual and equivalent filters are equal. Thus we require that

$$\int_0^{k_{1e}} \phi_1'(k_1) dk_1 = \int_0^\infty [\sin(k_1 c/2)/(k_1 c/2)]^2 dk_1,$$

or

$$k_{1e} = \pi/c, \quad (6.3)$$

and

$$\begin{aligned} \int_0^{\rho_e} \phi_2' \cdot \phi_3' \cdot \rho d\rho &= \frac{1}{2\pi} \int \exp[-\sigma^2(k_2^2 + k_3^2)] dk_2 dk_3 \\ &= \int \exp[-\sigma^2 \rho^2] \rho d\rho, \end{aligned}$$

or

$$\rho_e = 1/\sigma. \quad (6.4)$$

With the equivalent rectangular filter approximation, the following analytical expressions can be derived for

the longitudinal one-dimensional spectrum function:

$$\left. \begin{aligned} S_L'(k_1) &= \frac{\pi A}{2} \phi_1' \left\{ \frac{18}{55} \frac{1}{k_1^{5/3}} \right. \\ &\quad \left. - \frac{k_1^2}{(k_1^2 + \rho_e^2)^{11/6}} \left[ \frac{18}{55} + \frac{3}{5} \left( \frac{\rho_e}{k_1} \right)^2 \right] \right\}, \quad k_0 < k_1 \\ S_L'(k_1) &= \frac{\pi A}{2} \phi_1' \left\{ \frac{3}{5} \frac{1}{k_0^{5/3}} \left[ 1 - \frac{5}{11} \left( \frac{k_1}{k_0} \right)^2 \right] \right. \\ &\quad \left. - \frac{k_1^2}{(k_1^2 + \rho_e^2)^{11/6}} \left[ \frac{18}{55} + \frac{3}{5} \left( \frac{\rho_e}{k_1} \right)^2 \right] \right\}, \quad (\rho_e^2 + k_1^2)^{1/2} > k_0 > k_1 \\ S_L'(k_1) &= 0, \quad k_0^2 > \rho_e^2 + k_1^2 \end{aligned} \right\} \quad (6.5)$$

Eq. (6.5) is plotted in Fig. 5. It is seen that there is excellent agreement between the spectra corresponding to the actual and equivalent filters for wavenumbers larger than the cutoff wavenumber. At smaller wavenumbers, the equivalent filter approximation shows a sharp cutoff at large  $B$ . Under these conditions, the zero energy "hole" in the assumed spectrum occurs at a length scale smaller than the beam dimension, and so the equivalent filter spectrum cuts off sharply.

The behavior of the one-dimensional spectra may be understood qualitatively with reference to Fig. 6 which gives a graphical representation of the method of computing the one-dimensional spectrum. Two surfaces of constant  $\phi_{11}(\mathbf{k})$  are shown in Fig. 6. The spherical surface of radius  $k_0$  inside which  $\phi_{11}(\mathbf{k}) = 0$  is also shown. Now to find  $S_L(k_1)$  at any particular value of  $k_1$ , we first construct a plane at constant  $k_1$ , then multiply the values of  $\phi_{11}$  on this plane by the beam filter functions along  $k_2$  and  $k_3$ , and finally integrate these values with respect to  $k_2$  and  $k_3$  over the entire  $(k_2, k_3)$  plane. The result is  $S_L(k_1)$ . A cut by a plane  $k_1 = \text{constant}$ , and the values of  $\phi_{11}$  on this plane are shown schematically by the shading in Fig. 6. This graphical interpretation immediately shows the effect of the spherical "hole" on  $S_L(k_1)$ . For  $k_1 > k_0$  the plane at constant  $k_1$  does not intercept the spherical "hole" and, therefore, it does not have any effect on  $S_L(k_1)$ . For  $k_1 < k_0$ , the plane intercepts the hole and there is no contribution to  $S_L(k_1)$  from the region inside the hole, consequently  $S_L(k_1)$  is reduced below the value it would have if no hole was assumed. This shows why the full and dashed curves in Fig. 2 coincide for  $k_1 > 2\pi$  [ $\text{km}^{-1}$ ], and the dashed curves are below the full curves for  $k_1 < 2\pi$  [ $\text{km}^{-1}$ ]. The sharp fall-off in Fig. 2, and the sharp cutoff in Fig. 5, in the value of  $S_L(k_1)$  for  $k_1 < k_0$ , with increasing  $B$  can also be understood with reference to Fig. 6. With the equivalent rectangular filter approximation, the beam filter func-

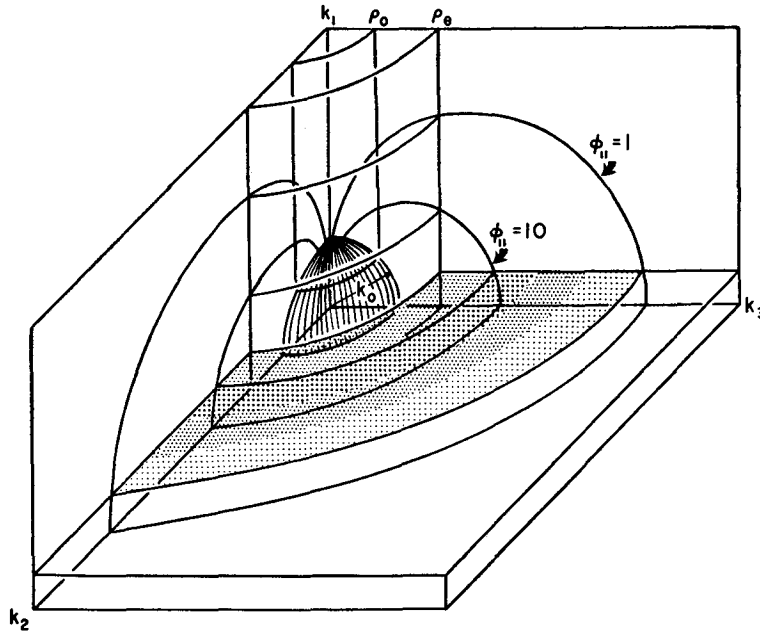


FIG. 6. Graphical representation of the computation of  $S_L(k_1)$ . Contours of  $\phi_{11}$  and the "hole" of radius  $k_0$  of zero energy are shown. The shaded plane is a cut at constant  $k_1$ , the intensity of the shading representing the value of  $\phi_{11}$  qualitatively. The cylinder  $\rho_e$  represents the equivalent rectangular filter in the  $(k_2, k_3)$  directions; only the region inside the cylinder contributes to  $S_L(k_1)$ . When the equivalent filter has radius  $\rho_0$ ,  $S_L(k_1)$  falls to zero.

tion in the  $k_2, k_3$  directions is such that values of  $\phi_{11}$  inside the cylinder

$$\rho = (k_2^2 + k_3^2)^{1/2} = \rho_e = 1/\sigma = 1/0.3003B$$

are multiplied by unity while values outside are multiplied by zero. Thus, only the region inside the  $\rho_e$  cylinder shown in the figure contributes to  $S_L(k_1)$ . As  $B$  increases  $\rho_e$  decreases and the region of the  $(k_2, k_3)$  plane contributing to  $S_L(k_1)$  decreases. When  $B$  is so large that  $\rho_e < k_0$  and the cylinder falls inside the spherical hole,  $S_L(k_1)$  drops to zero as in Fig. 5. This happens when the beam dimension corresponds to  $\rho_e = \rho_0$  shown in Fig. 6. With the actual filter, the beam-weighting does not fall to zero abruptly and therefore  $S_L(k_1)$  does not drop to zero abruptly but rather falls rapidly. The above discussion has been with reference to the longitudinal spectrum. A similar discussion can be given for the transverse spectrum by cutting the contours of  $\phi_{11}$  by a plane of constant  $k_2$  or  $k_3$ .

### 7. Concluding remarks

In this paper we deduced an equation [(3.10)] relating the average radial velocity measured by a Doppler radar to the point velocity measured by an ideal sensor, and an equation [(3.13)] relating the spectra of the average and point velocities. It is found that scales small compared to the beam dimensions are strongly attenuated while comparatively large scales are essentially unaffected when the three-dimen-

sional spectrum is considered. In the case of the one-dimensional spectra, scales large compared to the beam dimension are also attenuated, because small scales orthogonal to the direction, contributing to the one-dimensional spectrum, are attenuated. The total energy lost as a result of beam filtering appears as the variance of the Doppler spectrum (Rogers and Tripp, 1964). It is shown that, in general, the effects of filtering are not even poorly approximated by replacing the actual pulse volume by a sphere of equal volume, as has been proposed by other investigators. However, the actual beam filter functions may be replaced by equivalent rectangular filters without altering the results significantly. Moreover, the equivalent rectangular filter approximation enables analytical results to be obtained for the one-dimensional longitudinal spectrum.

*Acknowledgments.* The authors are indebted to Mr. R. S. Sekhon for help in the computations. Thanks are also due to Dr. J. Sychra for his contributions to Section 3a.

### REFERENCES

- Atlas, D., and R. C. Srivastava, 1971: A method for radar turbulence detection. *IEEE Trans. Aerosp. Electron. Syst.*, **7**, 179-187.
- Batchelor, G. K., 1953: *The Theory of Homogeneous Turbulence*. Cambridge University Press, 197 pp.
- Chernikov, A. A., Yu. V. Mel'nichuk, Z. N. Pinus, S. M. Shmeter and N. K. Vinnichenko, 1969: Investigations of the turbu-



- lence in convective atmosphere using radar and aircraft. *Radio Sci.*, **4**, 1257-1259.
- Gorelik, A. G., V. V. Kostarev and A. A. Chernikov, 1958: Radar measurements of turbulent motions in clouds. *Meteor. Gidrol.*, **5**, 12-19.
- , Yu. V. Mel'nichuk and A. A. Chernikov, 1963: The statistical characteristics of the radar echo as a function of the dynamic processes and microstructure of the meteorological entity. *Tr. Tsentr. Aerolog. Observ.*, No. 48, 3-54; AFCRL Transl. No. T-R-479, 91 pp.
- Lhermitte, R. M., 1968: Turbulent air motion as observed by Doppler radar. *Preprints 13th Radar Meteor. Conf.*, Montreal, Amer. Meteor. Soc., 498-503.
- Mel'nichuk, Yu. V., 1966: Measuring turbulence in precipitation with a doppler radar station. *Izv. Atmos. Oceanic Phys.*, **2**, 421-426.
- , G. A. Smirnova and A. A. Chernikov, 1968: Radar measurements of the rate of turbulent energy dissipation in clouds and precipitation. *Preprints 13th Radar Meteor. Conf.*, Montreal, Amer. Meteor. Soc., 486-489.
- Rogers, R. R., and B. R. Tripp, 1964: Some radar measurements of turbulence in snow. *J. Appl. Meteor.*, **3**, 603-610.
- Sychra, J., 1972: Inverse problem in the theory of turbulence filtering by the radar pulse volume. *Preprints 15th Radar Meteor. Conf.*, Urbana, Ill., Amer. Meteor. Soc., 286-291.
- Tatarskii, V. I., 1961: *Wave Propagation in a Turbulent Medium*. New York, Dover 285 pp.
- Wilson, D. A., 1970: Doppler radar studies of boundary layer wind profile and turbulence in snow conditions. *Preprints 14th Radar Meteor. Conf.*, Tucson, Ariz., Amer. Meteor. Soc., 191-196.